Renewable and Sustainable Energy Reviews 74 (2017) 1240–1256

Contents lists available at ScienceDirect

Renewable and Sustainable Energy Reviews

journal homepage: www.elsevier.com/locate/rser

Review and simulation of leakage current in transformerless microinverters for PV applications

Ahmad Khan*, Lazhar Ben-Brahim, Adel Gastli, Mohieddine Benammar

Department of Electrical Engineering, College of Engineering Qatar University, Doha, Qatar

ARTICLE INFO

Keywords:
Leakage current
Common Mode (CM)
PhotoVoltaic (PV)
Microinverter
Inverter
Pulse Width Modulation (PWM)
Transformerless

ABSTRACT

Designing microinverters without transformers enhances system efficiency and power density and reduces cost. However, the transformer removal results in loss of galvanic isolation that leads to leakage current circulation. Recently, there has been wide concern about this leakage current circulation and solutions have been proposed for its reduction. The objective of this paper is to investigate the circulating leakage current of different microinverters, its generation mechanism, and its mitigation techniques. In order to have an objective comparison between the different topologies and their leakage current mitigation techniques, simulations were carried out using identical system parameters and operating conditions for all topologies under investigation. The results show that among all the topologies that use additional switches to mitigate the leakage current, the HERIC NPC types and DC-based NPC microinverters produce the lowest leakage current. Furthermore, recent development in this area shows that the leakage current could be also mitigated with just passive filters.

1. Introduction

Recent studies on small scale grid-connected PV systems show the superiority of Microinverters PV Systems (MIPVS) over traditional String Inverters PV Systems (SIPVS) [1–3]. Specifically, the study in [1] compared two PV systems with the same power rating to evaluate the score of both systems based on the reliability, environmental effect, cost of loss, cost of installation, and safety aspects criteria. This study confirmed that MIPVS is better than the SIPVS in all comparison criteria. In addition, the MIPVS reaches breakeven cost faster than the SIPVS and provide better initial investment [4]. Furthermore, MIPVS outperform SIPVS in the annual energy yield by more than 5% [5,6]. The superiority of MIPVS is due to its modularity, DC bus elimination, and smaller power rating operation. Specifically, the modularity is achieved by the fact that the maximum power point tracking (MPPT) algorithm operates independently for each PV module. Therefore, unlike the SIPVS, the MIPVS exhibits more efficient MPPT operation under non-uniform solar radiation that makes them more suitable for non-flat rooftop PV application [7]. Also, since microinverters are attached at the back of the PV modules they have less DC wiring and the requirement for a DC bus is completely eliminated leading to reduced shock and arc hazards [1] and smaller size of the PV system. These features encourage individuals to start their own PV plant with a flexible future expandability option [5]. In addition, the cost of the installation is significantly reduced due to the less electrical expertise required for the installation of the MIPVS [8]. Furthermore, MIPVS designs are more intelligent and effective in detecting and localizing system components failures [9]. Eventually, the smaller power rating of microinverters allows the usage of smaller electrolytic capacitors; hence smaller failure rate and longer lifetime are achieved [10]. In fact, studies [8,10] revealed that is not possible to replace the electrolytic capacitor with a film capacitor in string inverters.

Grid-connected microinverters are classified as transformer or transformer-less microinverters based on the existence of galvanic isolation. Furthermore, galvanic isolation means that the grid ground is different than the PV system ground; galvanic isolation is realized practically with a transformer. In addition, these transformers can be utilized as voltage boosters. Also, transformers are either placed in the AC side with line frequency operation or in the DC side with high frequency operation. Unfortunately, line frequency transformers in microinverters are impractical because of their size. Similarly, the high frequency transformers also introduce extra losses. According to [11], removing the transformer from the inverter or microinverter achieves 1–2% higher efficiency, improves the power density and reduces the cost [12–14]. As a result, recent trends in microinverter development are concentrating on transformerless designs. However, this global move toward transformerless designs raised a safety flag regarding the loss of galvanic isolation and the amount of the circulating leakage current [15]. This leakage current is caused by the existence of the parasitic capacitance between the PV terminals and the ground.

* Corresponding author.
E-mail addresses: ak098168@qu.edu.qa (A. Khan), brahim@qu.edu.qa (L. Ben-Brahim), adel.gastli@qu.edu.qa (A. Gastli), mbenammar@qu.edu.qa (M. Benammar).

http://dx.doi.org/10.1016/j.rser.2017.02.053
Received 25 April 2016; Received in revised form 29 December 2016; Accepted 12 February 2017

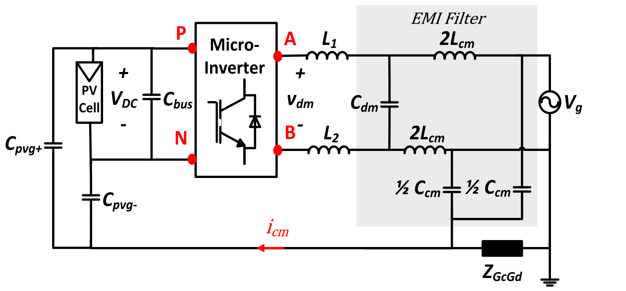

Fig. 1. Transformerless PV microinverter general circuit configuration with parasitic elements representation.

According to [16], the stray capacitance value ranges between 50-150nF/kWp for crystalline silicon cells and 1μF/kWp for thin film cells and it is dependent on temperature and climate conditions. In addition, leakage current circulation causes power losses, current harmonics, and electromagnetic interference [15,17]. Therefore, the suppression of this leakage current results in improving the reliability of the system [18].

Table 1
Parameters used in the study of the leakage current.

V_{DC}	V_g		f_o	$f_{swithcing}$
120 $\sqrt{2}$ V	120 Vrms		50 Hz	16 kHz
C_{pvg-}=C_{pvg+}	C_{bus}	C_o[a]	L_1=L_2	R_L
1.5 nF	3 mF	60 μF	0.85 mH	24 Ω

[a] LC common mode current elimination filter $C_o/2= C_{o1}= C_{o2}$.

Previously, PV systems grid-connection required satisfying specific standards such as IEC [19]. Most of these standards specify the power quality requirement, fault protection and detection requirement, and synchronization and reconnection requirement. New requirements have been added to the VDE German code about the maximum leakage current magnitude and its sudden variation [20]; if the leakage current is over 300 mA RMS or the sudden variation reaches 30 mA RMS then this should result in tripping the inverter from the grid irrespective of the power conversion level [21].

This paper explores (i) the leakage current generated by different-full bridge topologies of microinverters with different PWM schemes and (ii) the methodologies used to reduce the generated leakage current. The study excludes the family of half-bridge topologies because they need twice the grid peak voltage at the DC-link which stresses further the high gain boost DC-DC converter connected with the PV module [21–25]. Specifically, the paper compares the leakage current for different topologies based on the general circuit configuration shown in Fig. 1 and under the same environmental and operating conditions given in Table 1. Note that in order to simplify this analysis, the grid is replaced by a grounded resistive load R_L. Eventually, a ranking of these topologies is presented based on the magnitude of the leakage current RMS value.

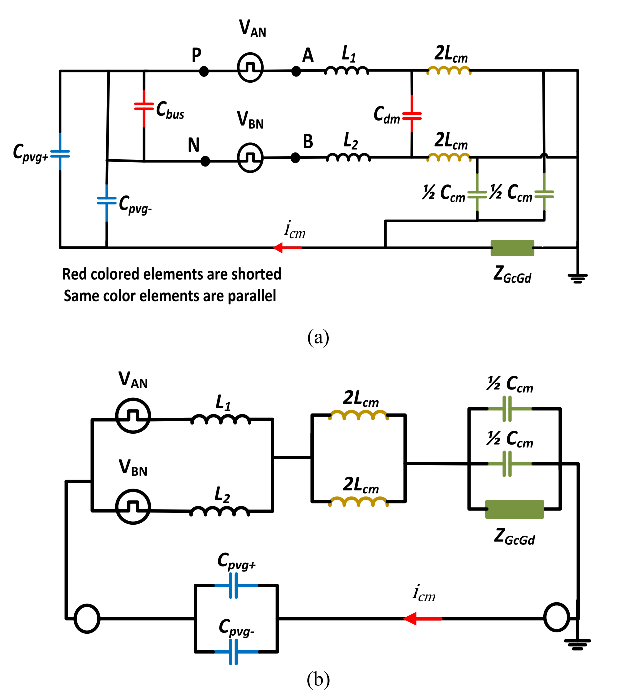

Fig. 2. Microinverter high frequency CM equivelent model: (a) steps to obtain the high frequency CM equivelent circuit and (b) the CM equivelent circuit.

2. Problem statement

2.1. Common Mode voltage

Without the galvanic isolation between the grid and the PV system, a Common Mode (CM) resonant circuit is formed. This CM circuit consists of the stray capacitances $C_{pvg+}$and C_{pvg-} between the PV panel terminals and ground, the impedance of the negative terminal of the grid and the ground of the PV panel Z_{GcGd}, and the EMI filter components shown in Fig. 1.

By analyzing the CM noise in Fig. 1, it is clear that the equivalent CM model can be represented as four different voltage sources, V_{DC}, v_g, v_{AN} and v_{BN}. The four distinct sources have different frequencies, hence superposition analysis must be considered. Nevertheless, the grid voltage and PV source can be ignored because of their low frequency content compared to the two CM noise sources v_{AN} and v_{BN} [26]. Also, because the CM current is of capacitive nature, high frequency signals are the major concern. Evidently any impedance connected in parallel with the neglected sources (e.g. C_{bus} in Fig. 1) is shorted. According to [26], C_{dm} does not affect the CM current and it is also shorted in the analysis. Consequently, the high frequency CM equivalent circuit can be represented as in Fig. 2(b) [27].

Using Thevenin's theorem, it is possible to find a general term for the total CM noise. Explicitly, according to Fig. 3(a), Z_{Th} is expressed as (1)

$$Z_{Th} = L_1//L_2 + 2L_{cm}//2L_{cm} + \frac{C_{cm}}{2}//\frac{C_{cm}}{2}//Z_{GcGd} \tag{1}$$

and according to Fig. 3(b), V_{Th} is the open circuit voltage at the C_{pvg+} and C_{pvg-} terminals (2).

$$V_{Th} = v_{total\_CM} = \frac{v_{AN}L_2 + v_{BN}L_1}{L_2 + L_1} \tag{2}$$

Notice that $(2L_{cm}//2L_{cm})$and $(\frac{C_{cm}}{2}//\frac{C_{cm}}{2}//Z_{GcGd})$ are in series with the stray capacitances C_{pvg+} and C_{pvg-}, so they are in open circuit condition during V_{Th} analysis. In other words, $(2L_{cm}//2L_{cm})$and $(\frac{C_{cm}}{2}//\frac{C_{cm}}{2}//Z_{GcGd})$ are in series with the open Thevenin terminals. As a result, V_{Th} is equivalent to the total CM voltage as in (2).

The voltages v_{AN} and v_{BN} may be written in terms of common mode and differential components, give (5) and (6) first, then: Considering the conventional CM voltage as (3)

$$v_{cm} = \frac{v_{AN} + v_{BN}}{2} \tag{3}$$

and the differential mode voltage as (4)

$$v_{dm} = v_{AN} - v_{BN} \tag{4}$$